# Skin and proximity effects analysis in split gradient coils

Fangfang Tang[1], Hector Sanchez Lopez[1], Fabio Freschi[2], Feng Liu[1], and Stuart Crozier[1]
[1]*School of Information Technology and Electrical Engineering, The University of Queensland, Brisbane, Queensland, Australia,* [2]*Politecnico di Torino Corso Duca Degli Abruzzi, Department of Energy, Torino, Italy*

**Introduction:** In MRI, eddy currents are induced by the inductive interaction between the gradient coils and surrounding metallic conductors. These eddy currents inevitably distorts the primary field, produces imaging artifacts, acoustic noise and is the cause of power loss in the cryostat and radiofrequency (RF) shield[1]. In this paper, we extended the multi-layer integral method (MIM) [2] to study the skin and proximity effects in and between the gradient coils tracks and between the gradient coils conductors and the surroundings.

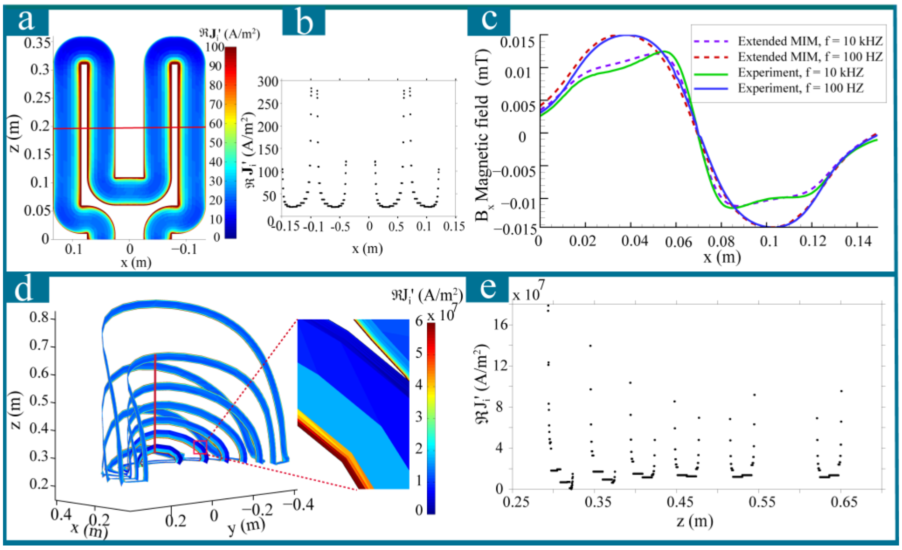


**Method:** To study the study the skin and proximity effects using the MIM method, an anisotropic mesh was used to discretize the coil tracks. The width division was smaller than the skin depth in order to accurately account the skin effect. Moreover the conductors were assumed thin enough to keep the current density uniform along the normal direction of the coil track. The gradient coil conductor is represented by a domain Ω' where **r**'∈Ω' but **r**'∉Ω; and **r**∈Ω. An eddy current $\mathbf{J}_i(\mathbf{r},\omega)$ that flows in the conducting domain Ω is induced by the alternating current $\mathbf{J}_i'(\mathbf{r}',\omega)$. $\mathbf{J}_i(\mathbf{r},\omega)$ flows only in the domain Ω but not in the domain Ω' and no current flow between domain Ω and domain Ω'. Both domains are inductively coupled and the condition $\nabla\cdot\mathbf{J}_i(\mathbf{r},\omega)=0$ and $\nabla\cdot\mathbf{J}_i'(\mathbf{r}',\omega)=0$ holds for both domains. Therefore the diffusion equation for the time-harmonic current density used in MIM $(i\omega\mathbf{M}_{ii}+\mathbf{R}_{ii})\mathbf{\Psi}_i=-i\omega\mathbf{M}_{is}\mathrm{I}_0$ is modified to $(i\omega\mathbf{M}_{ii}+\mathbf{R}_{ii})\mathbf{\Psi}_i=0$, where $\mathbf{R}_{ii}$ is resistive term and $\mathbf{M}_{ii}$ is inductive coupling. The matrix $\mathbf{M}_{ii}$ includes the inductive interaction of all the elements belonging to the domains Ω' and Ω and the mutual interaction between both domains; but $\mathbf{R}_{ii}$ includes the terms of resistive interactions, acting locally among adjacent elements. $\mathbf{\Psi}_i$ is the unknown stream function in the domains Ω' and Ω, respectively. We assume $\mathbf{A}=\ i\omega\mathbf{M}_{ii}+\mathbf{R}_{ii}$, so $\mathbf{A}\mathbf{\Psi}_i=0$. $\mathbf{\Psi}_i$ is divided in two sets: $\mathbf{\Psi}_i=\begin{bmatrix}\mathbf{\Psi}_i^{\Omega,\Omega'}\\ \mathbf{\Psi}_0^{\Omega,\Omega'}\end{bmatrix}$, where $\mathbf{\Psi}_i^{\Omega,\Omega'}$ are the vector containing values of the stream function of the internal nodes in domains Ω' and Ω. $\mathbf{\Psi}_0^{\Omega,\Omega'}$ contains the values of the nodes of the domain boundaries. $\mathbf{\Psi}_i^{\Omega,\Omega'}$ is solved from the transformation formula $\begin{bmatrix}\mathbf{A}_{\Omega,\Omega'} & \mathbf{A}_{\Omega,\Omega'0}\\ \mathbf{A}_{0\Omega,\Omega'} & \mathbf{A}_0\end{bmatrix}\begin{bmatrix}\mathbf{\Psi}_i^{\Omega,\Omega'}\\ \mathbf{\Psi}_0^{\Omega,\Omega'}\end{bmatrix}=\begin{bmatrix}0\\0\end{bmatrix}$ of $\mathbf{A}\mathbf{\Psi}_i=0$. Assuming that $\mathbf{A}_0$is the impedance matrix for those nodes belonging to the domains boundaries, $\mathbf{A}_{\Omega,\Omega'0}$ is the interaction of the edges nodes (with known stream function values ) with the internal nodes and $\mathbf{A}_{\Omega,\Omega'}$ is the interaction between the internal nodes of the domains Ω' and Ω. Once $\mathbf{\Psi}_i$ is calculated, the current densities $\mathbf{J}_i(\mathbf{r},\boldsymbol{\omega})$ and $\mathbf{J}_i'(\mathbf{r}',\boldsymbol{\omega})$ are evaluated, and then the parameters such as power loss, force and magnetic field and spherical harmonics in the DSV are evaluated.

In order to demonstrate that the extended MIM accurately reproduce the skin and proximity effects, an arbitrary coil showed in Figure a) was designed using GMSH. We assumed a 0.75mm copper sheet. The width of the coil was set to 27cm and the height 36cm along the *z*-axis. The vertical straight part (along *x*-axis) was designed long enough to avoid effects from the transverse part (along *z*-axis). Both the central gap and the width of the coil track were set to 50mm and the smaller gap to 10mm. An anisotropic mesh was used to cope with the skin and proximity effects. The arbitrary coil was simulated with extended MIM using two frequencies 100 Hz and 10 kHz. The stream function was set to 2A at the nodes belonging to one side of the coil. The opposite side was grounded to zero in order to produce a current flow along one direction. To compare with the results simulated from extended MIM, an experiment was set up and an amplifier was used to produce a current 2A to drive the coil at the target frequencies. The magnetic field Bx(x) was measured from x=-15cm to x = 0 at z=18.5cm along the red line showed in Figure a). The measured Bx(x) was compared with that predicted by extended MIM.

The extended MIM was used to analyze a more complex coil. A split 24 turns *x*-gradient coil with a simplified cold shield was designed [3] and simulated using the extended MIM to study the skin and the proximity effect. The field linearity was constrained to 5% within a 300 mm DSV and the target gradient strength was $G_0$=10mT/m. The gap between the coil tracks was 2.8mm.

**Results and Discussions:** Figure a) presents the colormap of the current density magnitude at frequency 10 kHz and Figure b) shows the current density distribution along the red line in Figure a). Both Figures a) and b) illustrate that the current density in the inner edge is higher than the outer edge due to the proximity effect between the two inner edges. Figure c) describes the magnetic fields predicted by extended MIM and that measured in the experiment at frequencies 100 Hz and 10k Hz. The arbitrary coil was discretised into 24798 triangles and the simulation took 7 mins using an Intel® Core(TM) i7 CPU with 16 GB of RAM. The result shows that the measured value and the result predicted by extended MIM have a good agreement for both frequencies. Figure c) illustrates a "double-hump" shape due to the tendency of the current density to increase at the edges. The double-hump is asymmetric due to the higher current density at the inner edge than the outer edge. The symmetric of field profile for 100 Hz corresponds to a uniform current density profile along the track width.

We chose the average power loss $\frac{1}{2}\mathbf{\Psi}_i\mathbf{R}_{ii}\mathbf{\Psi}_i{}'$ as a convergence criterion in order to select an optimal number of divisions along the coil track of the *x*-gradient coil. We found 10 to be the optimal number of divisions. The number of nodes of the designed split *x*-gradient coil was 30349 and the simulation took 22 mins for divisions 10 on each track. Figure e) shows the colormap of the current density profile of the designed *x*-coil at the frequency of 10 kHz. The current density distribution along the track width is asymmetric and this effect is more emphasised on coil tracks with a rapid spatial behaviour. Tracks with rapid variation have a higher current density distribution and exhibit more asymmetries than the track width with smooth current paths. Figure e) presents the spatial current density distribution along the red line in Figure d), which exhibits the track close to the coil "eye" produce a higher current density and power loss than smoother tracks.

**Conclusions:** The extended MIM method was experimentally validated for the investigation of skin and proximity effects for a demonstration coil for frequencies up to 10 kHz. It was demonstrated that the rapid current paths should be avoided in order to mitigate asymmetric current density profile and power loss. The method opens the possibility of understanding the interactions between the coil tracks and the consequences on power loss and the effect of the coil track width over the field harmonics in the DSV. The extended MIM can be used to investigate how much error is introduced in the coil evaluation when the coil is evaluated as an infinitely thin wire segments and what are the consequences of the approach over the calculation of parameters such as the power loss in the cryostat, field harmonics produced by the coil and cryostat, inductance and resistance calculation in regards of the frequency and track width.

**References:** [1]C. Boesch, R. Gruetter, and E. Martin, Magnetic resonance in medicine, vol. 20, pp. 268-284, 1991. [2]H. Sanchez Lopez, F. Freschi, A. Trakic, E. Smith, J. Herbert, M. Fuentes, et al., Magnetic Resonance in Medicine, 2013. [3] H. Sanchez, et al J Magn Reson, 199, 48-55, (2009)